Dalton Transactions

PAPER

View Article Online
View Journal | View Issue

Cite this: *Dalton Trans.*, 2018, **47**, 2360

The effect of metal distribution on the luminescence properties of mixed-lanthanide metal–organic frameworks†

Laura K. Cadman, Mary F. Mahon* and Andrew D. Burrows *

A series of lanthanide metal–organic frameworks (MOFs) of the general formula [Ln(Hodip)(H_2O)]·$n$$H_2O$ (Sm, **1**; Eu, **2**; Gd, **3**; Tb, **4**; Dy, **5**; Er, **6**; H_4odip = 5,5′-oxydiisophthalic acid) have been prepared and shown crystallographically to have isostructural three-dimensional frameworks. The fluorescence emission spectra of the europium compound **2**, which is red, and the terbium compound **4**, which is green, show characteristic peaks for transitions involving the metal centres, whereas that for the gadolinium compound **3** is dominated by transitions involving Hodip. Using a 1 : 1 : 1 mixture of europium, gadolinium and terbium nitrates in the synthesis resulted in the mixed-metal MOF [$Gd_{0.17}Tb_{0.19}Eu_{0.64}$(Hodip)($H_2O$)]·$n$$H_2O$ **7**, for which the ratio of the metal ions was determined using EDX spectroscopy. The fluorescence emission spectrum of **7** is dominated by europium emission bands reflecting the higher proportion of Eu^{3+} centres and quenching of the terbium fluorescence by metal-to-metal energy transfer. A series of core–shell MOF materials based on the Ln(Hodip)(H_2O) framework have been prepared in order to isolate the lanthanides in different domains within the crystals. The emission spectra for materials with Gd@Tb@Eu (**8**) and Tb@Eu@Gd (**9**) are dominated by terbium emissions, suggesting that physical separation from europium suppresses quenching. In contrast, the material with Eu@Gd@Tb (**10**) shows only broad ligand bands and europium emissions. This confirms that core–shell MOFs have different fluorescence properties to simple mixed-metal MOFs, demonstrating that the spatial distribution of the metals within a mixed-lanthanide MOF affects the fluorescence behaviour.

Received 5th December 2017,
Accepted 17th January 2018

DOI: 10.1039/c7dt04583b

rsc.li/dalton

Introduction

Metal–organic frameworks (MOFs) that contain lanthanide centres generally display different topologies and properties from those of the d-block metals. The larger ionic radii of lanthanide ions results in high coordination numbers, and this in turn can lead to high connectivity, hence facilitating the formation of stable three-dimensional networks, despite the high ionic character of the metal–ligand bonds.[1,2]

The luminescent properties of lanthanide MOFs have attracted considerable attention recently due to potential lighting and sensing applications.[3–5] Emissions from discrete Ln^{3+} ions are generally sharp and of low intensity, but on complexation with an organic ligand the luminescence can be significantly enhanced. In this sensitisation process, the ligands act as antennae, absorbing UV photons to excite electrons, then transferring the excitation energies to the lanthanide(III) centres. This process is reliant upon the excited triplet state of the ligand being higher in energy than the excited state of the lanthanide ion. The high thermal stability of lanthanide MOFs, coupled with the enhancement of luminescent properties by organic linkers, makes these materials attractive for a range of applications including those involving second harmonic generation[6] and temperature sensing.[7–9] The porosity of MOFs means that these materials are also promising candidates for other applications such as chemical sensing.[2,10–13]

The emission properties of a lanthanide MOF can be tailored by ligand design, in order to enhance the antenna effect, or through changing the guest molecules included within the pores.[4] Alternatively, combining lanthanides, especially Eu^{3+} (red) and Tb^{3+} (green), within the same material has proven effective in tuning the wavelength of the emission from MOF materials, either in the visible[14,15] or the near infrared[16] parts of the spectrum. Although this can be done by physically mixing materials, many lanthanide MOFs form isoreticular series,[17] whereby different lanthanide metals form isostructural materials. As a consequence, using a mixture of lanthanide ions in the synthesis can lead to mixed-metal MOFs.[18] For example, Guo and co-workers reported a series of MOFs with the general formula [$Eu_{1-x}Tb_x$(btc)(H_2O)] (btc = 1,3,5-benzenetricarboxylate)

Department of Chemistry, University of Bath, Claverton Down, Bath BA2 7AY, UK. E-mail: a.d.burrows@bath.ac.uk

† Electronic supplementary information (ESI) available: Synthetic and characterisation details, X-ray crystal structures. CCDC 1586990–1586995. For ESI and crystallographic data in CIF or other electronic format see DOI: 10.1039/c7dt04583b

and varying Eu : Tb ratios. The structures show a change in the intensity of the Tb^{3+} emission with alterations in the Eu : Tb ratio. As a result, the mixed-lanthanide structures range in colour from yellow/green to red,[19] whereas other systems have been developed to emit white light.[20–22]

Mixed-lanthanide MOFs typically have a random distribution of the lanthanide centres throughout the structure. This randomisation can lead to quenching of the colour emissions through energy transfer between emitter centres, making colour control difficult to achieve. One method to overcome this quenching is to form ordered, heterogeneous structures in which the different emitters are located within specific regions of the structure. This has been demonstrated through the formation of core–shell mixed-lanthanide systems based on the frameworks of $[Ln_2(bhc)(H_2O)_8]\cdot H_2O$ (bhc = benzene-1,2,3,4,5,6-hexacarboxylate).[23]

While studies on lanthanides MOFs containing rigid linkers are relatively common, there have been few reported on comparative systems with inherent linker flexibility.[24] In order to investigate this unexplored area, the formation of lanthanide MOFs using 5,5′-oxydiisophthalic acid (H_4odip, Fig. 1) was investigated. H_4odip has the potential to act as a tetracarboxylate ligand following deprotonation of all its carboxylic acid groups and has a flexible ether bridging group between the benzene rings. Indeed, H_4odip has previously been used to prepare MOFs based on d- and p-block metals,[25,26] but no lanthanide MOFs using this linker have been reported to date.

In this paper, we describe the formation of lanthanide-Hodip MOFs using samarium(III), europium(III), gadolinium(III), terbium(III), dysprosium(III) and erbium(III). The products were structurally characterised through single crystal and powder X-ray diffraction methods, and the luminescence properties of the products were analysed through fluorescence spectroscopy. The possibility of tuning the emission of the lanthanide-Hodip-containing frameworks was investigated through the synthesis of isostructural, mixed-lanthanide materials, through employing several metal salts in the synthesis and also through the formation of core–shell materials. The fluorescence spectra of these mixed-metal materials are compared to those of physical mixtures of single-lanthanide MOFs.

Results and discussion

Synthesis and structural analysis

Reactions between the hydrated lanthanide nitrate salts, $Ln(NO_3)_3\cdot xH_2O$, with H_4odip were carried out in water at 85 °C for 48 h. In all cases the reactions yielded colourless, crystalline water-stable products that were identified as $[Ln(Hodip)(H_2O)]\cdot nH_2O$ (Ln = Sm, **1**; Eu, **2**; Gd, **3**; Tb, **4**; Dy, **5**; Er, **6**).

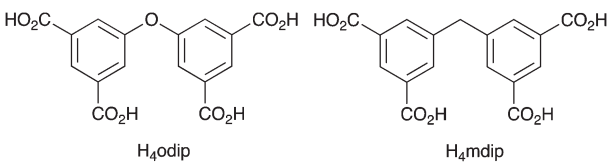

Fig. 1 The structure of H_4odip, in comparison to that of H_4mdip.

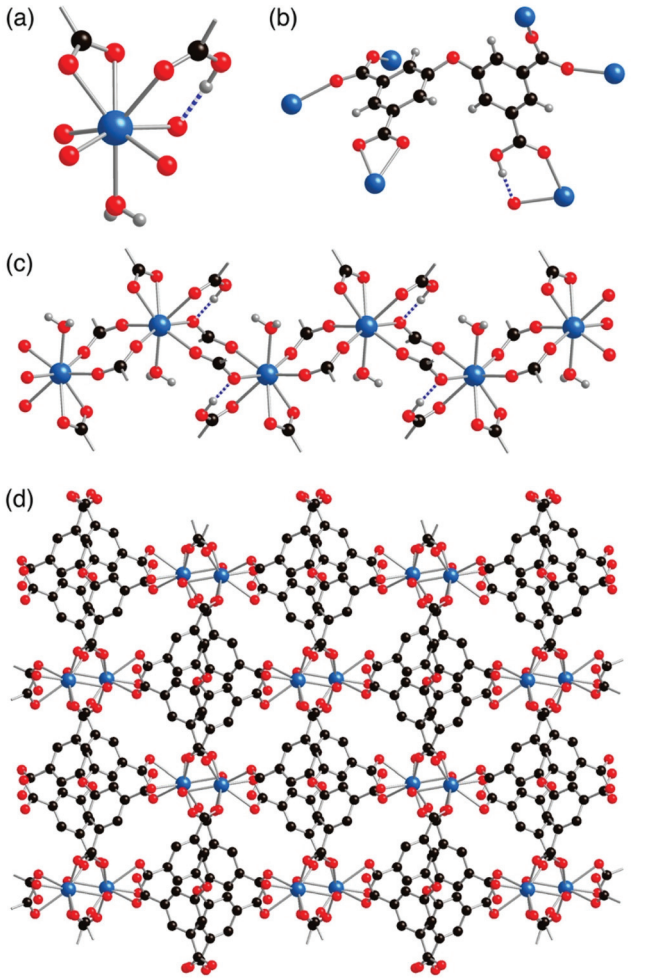

Fig. 2 The crystal structure of $[Tb(Hodip)(H_2O)]\cdot 2H_2O$ **4**, showing (a) the metal coordination sphere, (b) the bridging Hodip lignd, (c) the carboxylate-bridged chains running along the *a*-axis, and (d) the gross structure, with hydrogen atoms and included water molecules omitted for clarity.

Crystals of **1** and **3–6** were suitable for single crystal X-ray diffraction analysis.‡ The five compounds were isostructural, and the description herein is limited to the terbium compound **4**. The asymmetric unit of **4** is formed from one terbium centre, one singly-protonated Hodip ligand, one water molecule coordinating to the Tb centre and two included water molecules, one of which is disordered over two positions. The terbium centre is eight-coordinate (Fig. 2a),

‡Crystal data for $C_{16}H_{13}O_{12}Tb$ (**4**): M = 556.18 g mol^{-1}, monoclinic, space group $P2_1/n$ (no. 14), a = 9.8243(2), b = 12.7350(3), c = 13.9772(3) Å, β = 93.8140(19)°, U = 1744.85(7) Å^3, Z = 4, T = 150(2) K, $\mu(CuK_\alpha)$ = 20.585 mm^{-1}, D_{calc} = 2.117 g cm^{-3}, 7002 reflections measured (9.404° ≤ 2θ ≤ 145.672°), 3383 unique (R_{int} = 0.0304) which were used in all calculations. The final R_1 was 0.0382 ($I > 2\sigma(I)$) and wR_2 was 0.0824 (all data).

bonding to six different Hodip ligands and one water molecule. Each Hodip ligand coordinates to six terbium atoms (Fig. 2b), one carboxylate group binding in a κ^2- mode, two bridging between metal centres and the fourth, which remains protonated, coordinating through a single oxygen atom, but supported by a short hydrogen bond between the carboxylic acid proton and a coordinated carboxylate oxygen atom in an intramolecular ring designated by the graph set S(6)[27] [O(9)···O(4) 2.591 Å, H(9)···1.64 Å, O(9)–H(9)···O(4) 177°]. The terbium centres are inter-connected through pairs of bridging carboxylate groups into 1D chains along the *a*-axis (Fig. 2c). These chains are linked together by the Hodip ligands to form a three-dimensional network (Fig. 2d).

The network contains small pores which are occupied by the included water molecules. The disordered water molecules, based on O(12)/O(12A), have site occupancies of 80% and 20% respectively, based upon electron density. The hydrogen atoms relating to these water molecules could not be reliably located and were therefore omitted from the refinement.

The X-ray analyses reveal differences in the occupation of the included solvent, and confirm the identity of the products as [Sm(Hodip)(H_2O)]·1.65H_2O **1**, [Gd(Hodip)(H_2O)]·2H_2O **3**, [Tb(Hodip)(H_2O)]·2H_2O **4**, [Dy(Hodip)(H_2O)]·1.8H_2O **5** and [Er(Hodip)(H_2O)]·1.8H_2O **6**. Single crystal X-ray analysis was not possible for the europium compound due to low crystal quality, so its formula is represented as [Eu(Hodip)(H_2O)]·*n*H_2O **2**.

Powder X-ray diffraction analyses for **1–6** are shown in Fig. 3. These patterns show that the compounds are isostructural, in accord with the X-ray single crystal findings, though the presence of a broad peak at ~12° in several cases suggests the co-presence of an amorphous phase. The experimental powder X-ray patterns are similar to those simulated from the single crystal structures, confirming the presence of a single crystalline phase in all cases.

The chain and gross structures of **4** (Fig. 2c and d) are similar to those observed in the methylenediisophthalate (mdip, Fig. 1) analogue (NMe_2H_2)[Tb(mdip)(H_2O)],[24] despite the fact that this framework is anionic, with the ligand fully deprotonated and the charge balanced by included dimethylammonium ions. In (NMe_2H_2)[Tb(mdip)(H_2O)], the terbium(III) centre is nine-coordinate, with the coordinated carboxylic acid group in **4** replaced by a κ^2-carboxylate. The angle between the two benzene rings of the Hodip ligand in **1** and **3–6** is 72° in all structures, which is greater than that observed in H_4odip·H_2O (52°, for details of this structure see ESI†) and comparable to the equivalent angle in (NMe_2H_2)[Tb(mdip)(H_2O)] (68°).

Fluorescence spectroscopy studies of H_4odip and [Ln(Hodip)(H_2O)]·*n*H_2O (Ln = Eu, Gd, Tb)

The solid-state fluorescence excitation and emission spectra of H_4odip are shown in Fig. 4. The excitation spectrum, produced with λ_{ex} = 420 nm, shows a broad band centred around 370 nm. The emission spectrum was recorded using an excitation wavelength equivalent to the excitation maximum (λ_{ex} = 370 nm) and shows a broad band centred at 420 nm. This arises from π–π* transitions and gives the compound an overall blue emission.

Fluorescence studies were conducted on samples of **2** and **4** due to the characteristic emissions of Eu^{3+} (red) and Tb^{3+} (green) in the visible region. The fluorescence activity of **3** was also investigated, as for Gd^{3+}-containing compounds this is often dominated by ligand emission. This is because the lowest excited (emitting) level in Gd^{3+} typically lies above the excited triplet level of organic ligands.[28]

The solid-state fluorescence excitation and emission spectra of **2**, **3** and **4** are shown in Fig. 5. The excitation spectra of the europium MOF **2** and the gadolinium MOF **3** are dominated by a broad band at 370 nm similar to that observed for H_4odip. The emission spectrum of **2** shows three peaks at 594 nm, 615 nm and 693 nm, which correspond to the $^5D_0$–$^7F_1$, $^5D_0$–$^7F_2$ and $^5D_0$–$^7F_4$ transitions of Eu^{3+}, respectively.[1] The Eu^{3+} transitions are overlapped by the broad emission band which is indicative of luminescence sensitisation of the Eu^{3+} centres by the ligand. The emission spectrum of **3** shows only the ligand emission, indicating no ligand sensitisation is occurring, which is consistent with the high energy of the Gd^{3+}

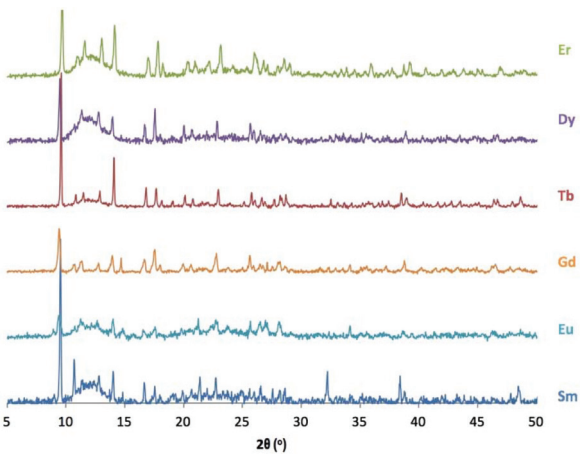

Fig. 3 Powder X-ray diffraction patterns for [Ln(Hodip)(H_2O)]·*n*H_2O (Ln = Sm, **1**; Eu, **2**; Gd, **3**; Tb, **4**; Dy, **5**; Er, **6**).

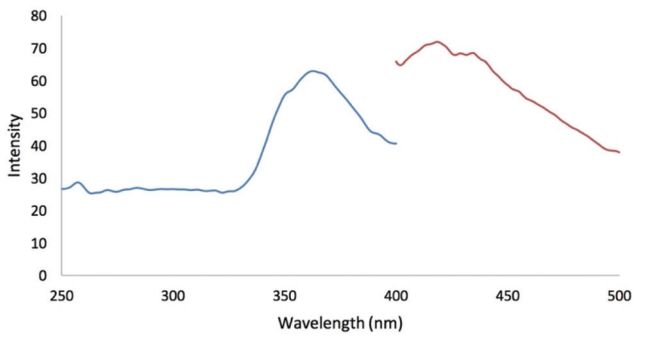

Fig. 4 The solid-state fluorescence emission (red) and excitation (blue) spectra of H_4odip. The emission spectrum was recorded using λ_{ex} 370 nm, and the excitation spectrum was produced with λ_{ex} 420 nm.

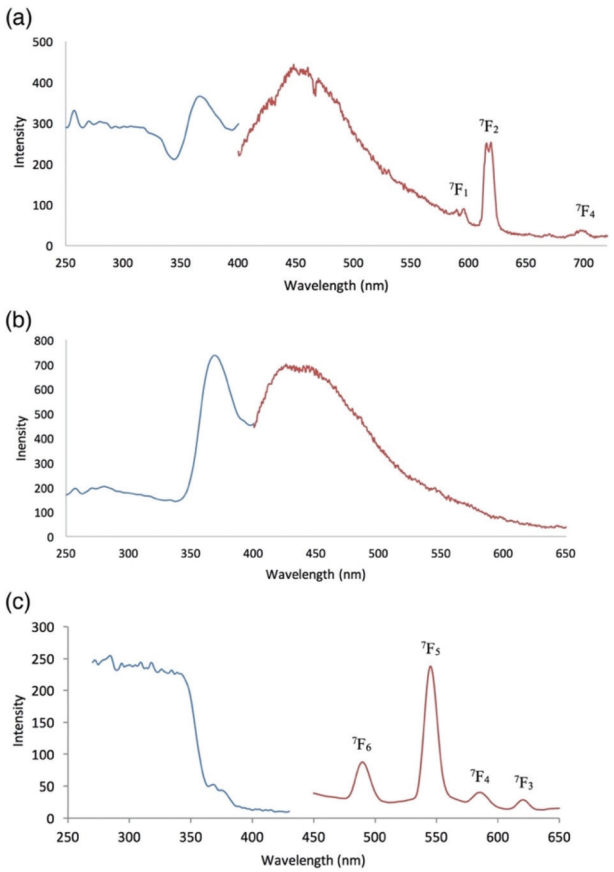

Fig. 5 Solid-state emission (red) and excitation (blue) spectra for (a) Eu(Hodip)(H_2O)·$n$$H_2O$ **2**, (b) Gd(Hodip)(H_2O)·2H_2O **3**, (c) Tb(Hodip)(H_2O)·2H_2O **4**. The emission spectra for **2** and **4** show the term symbols for the terminus of each transition. These originate from $^5D_0$ (for Eu^{3+}) and $^5D_4$ (for Tb^{3+}).

excited states.[28] The emission spectrum of the terbium MOF, **4**, shows four peaks at 480 nm, 545 nm, 580 nm and 620 nm which correspond to the $^5D_4$–$^7F_6$, $^5D_4$–$^7F_5$, $^5D_4$–$^7F_4$ and $^5D_4$–$^7F_3$ transitions between energy level states of Tb^{3+} respectively.[1]

The excitation spectra of **2–4** show similar features and are dominated by bands whose high intensity and broad nature is suggestive of ligand to metal charge transfer (LMCT). Such transitions are consistent with ligand sensitisation of the metal centres.[24] Similar bands have been observed in the excitation spectra of other lanthanide materials, but are absent from the spectra of simple lanthanide salts.[29]

Overall, the emissions of **2–4** are observed in the red, blue and green regions of the visible spectrum, respectively. The potential therefore exists to produce compounds which have colour-tuned emissions by combining these metal centres to produce mixed-lanthanide frameworks with the Hodip linker.

The mixed-lanthanide species [$Gd_{0.17}Tb_{0.19}Eu_{0.64}$(Hodip)($H_2O$)]·$n$$H_2O$

A mixed-metal MOF with the Ln(Hodip)(H_2O) framework was prepared by combining the nitrates of gadolinium, terbium and europium in a 1 : 1 : 1 ratio with H_4odip in H_2O and heating to 85 °C for 48 h. The reaction yielded a colourless crystalline product, **7**, which was analysed by powder X-ray diffraction and shown to be poorly crystalline, though the peak positions were consistent with those observed for **1–6** (Fig. S2†). The presence of Gd, Tb and Eu in **7** was confirmed by EDX spectroscopy. Scanning electron microscope (SEM) images of the sample show that the product is not homogeneous, with some particles appearing darker than others (Fig. 6).

The dark coloured particles correspond to materials which contain only light elements, and EDX analysis identified these as an organic material, most likely H_4odip. The lighter particles contain europium, gadolinium and terbium ions. Five of these particles were analysed by EDX spectroscopy to determine the percentage of the different lanthanides present, and the analyses gave average metal compositions of 63.9(13)% Eu, 19.4(4)% Tb and 16.7(12)% Gd. This gives an average formula for **7** of [$Eu_{0.64}Gd_{0.17}Tb_{0.19}$(Hodip)($H_2O$)], omitting included water molecules. The five crystallites that were analysed contained similar lanthanide ion ratios suggesting that little compositional variation is present (see ESI† for further details).

Visual observations of **7** under a UV lamp showed the product to be red when illuminated with light of λ = 254 nm. Solid-state fluorescence emission spectra were therefore recorded at room temperature through excitation at this wavelength (λ_{ex} = 254 nm) and at excitation of the ligand (λ_{ex} = 370 nm) and these are shown in Fig. 7a.

Both emission spectra are dominated by the high intensity emission bands of Eu^{3+} at 594 nm and 618 nm. Some evidence of Tb^{3+} emission is present, with a band at 545 nm, and the tail of the broad ligand emission band can also be observed (400–500 nm), which suggests sensitisation of the Ln^{3+} luminescence.

The excitation spectra were recorded through excitation of the ligand (442 nm), Tb^{3+} (545 nm) and Eu^{3+} (618 nm) and are shown in Fig. 7b. Excitation of Eu^{3+} shows a strong, broad

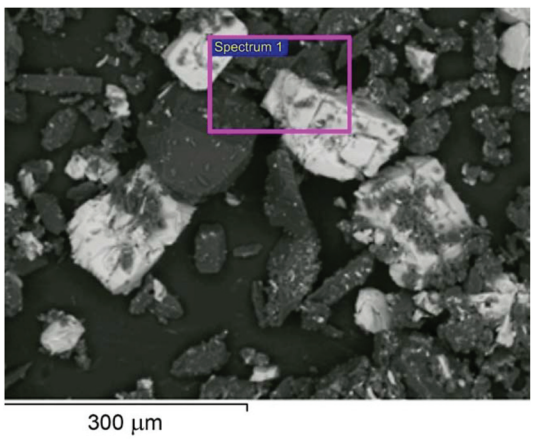

Fig. 6 SEM image of the product **7** formed from the reaction between H_4odip and a 1 : 1 : 1 mixture of Eu(NO_3)$_3$·$n$$H_2O$, Gd($NO_3$)$_3$·6$H_2O$ and Tb(NO_3)$_3$·5H_2O.

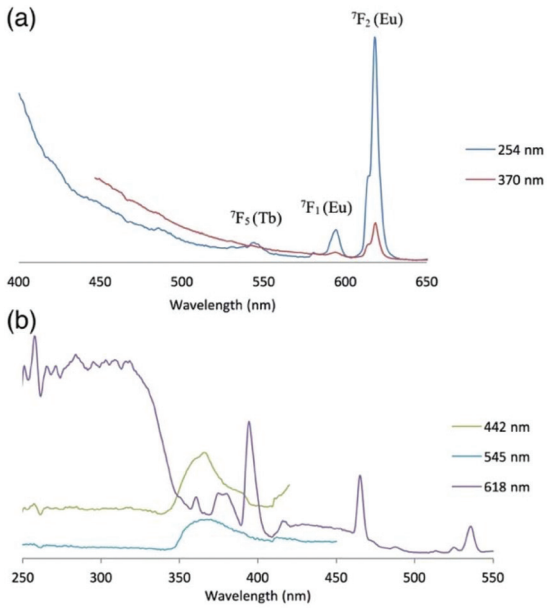

Fig. 7 The solid-state fluorescence (a) emission and (b) excitation spectra for $[Eu_{0.64}Gd_{0.17}Tb_{0.19}(Hodip)(H_2O)]\cdot nH_2O$ **7**.

band at 250–350 nm, likely due to LMCT, and sharper bands at 361 nm, 377 nm, 394 nm and 465 nm, which arise from Eu^{3+} transitions. The excitation of Tb^{3+} and the H_4odip have similar features to one another, both showing a broad band at 250–340 nm with a lower intensity to that of the analogous band in the Eu^{3+} excitation spectra, and a band at 370 nm characteristic of the ligand.

Overall, the solid-state fluorescence emission and excitation spectra of the mixed-lanthanide framework **7** shows a dominance by Eu^{3+}, which confirms the visual observations as the sample appears red under UV irradiation. This is likely to be due to the higher concentration of europium within the sample in comparison to terbium and gadolinium, but may also reflect quenching of the terbium fluorescence by the europium centres. Metal to metal energy transfer is known to occur between Tb^{3+} and Eu^{3+} ions in close proximity to one another.[23] Electrons in the excited states of Tb^{3+} are transferred to lower lying Eu^{3+} states, resulting in a quenching of Tb^{3+} transitions and a predominance of the Eu^{3+} transitions. Similar observations were made for mixed-lanthanide systems based on $[Ln_2(bhc)(H_2O)_8]\cdot H_2O$.[23]

Mixed-lanthanide core–shell species

The formation of core–shell lanthanide MOFs has previously been shown to prevent energy transfer between lanthanide ions within a mixed-metal system.[23] In order to explore whether that was the case for lanthanide-Hodip MOFs, three core–shell species were prepared through growth of one lanthanide-containing MOF onto the surface of a MOF with similar topology but containing a different lanthanide. The materials prepared in this manner were [Gd(Hodip)(H_2O)]@[Tb(Hodip)(H_2O)] @[Eu(Hodip)(H_2O)] **8**, [Tb(Hodip)(H_2O)]@[Eu(Hodip)(H_2O)] @[Gd(Hodip)(H_2O)] **9**, and [Eu(Hodip)(H_2O)]@[Gd(Hodip)(H_2O)]@[Tb(Hodip)(H_2O)] **10**. Compounds **8–10** each possess three domains, one containing each of europium, terbium or gadolinium centres. Overall, the three materials differ only in the ordering of the domains.

For **8**, $[Eu(Hodip)(H_2O)]\cdot nH_2O$ was first synthesised through the reaction of europium(III) nitrate with H_4odip in water at 85 °C for 48 h. The resulting crystals were decanted from the supernatant and placed in fresh water three times over 72 h to remove any unreacted reagents. The $[Eu(Hodip)(H_2O)]\cdot nH_2O$ crystals were placed in an aqueous solution of terbium(III) nitrate and H_4odip and heated to 85 °C for 48 h to form [Tb(Hodip)(H_2O)]@[Eu(Hodip)(H_2O)]. The resulting core–shell crystals were washed with water, then placed in an aqueous solution of gadolinium(III) nitrate and H_4odip and heated to 85 °C for a further 48 h to form the final core–shell structure. The other core–shell materials **9** and **10** were prepared in a similar manner but varying the order of treatment with the lanthanide reagents. Compounds **8–10** were all isolated as colourless crystalline materials.

Powder X-ray diffraction analyses on **8–10** revealed them to be isostructural with **1–6** (Fig. S4†), though **9** was of lower crystallinity than **8** and **10**. EDX spectroscopy was carried out on **8–10**, with four or five particles of each analysed for their gadolinium, europium and terbium content. This gave average lanthanide compositions of 82.2(76)% Gd, 14.3(14)% Tb and 3.6(9)% Eu for **8**, 88.6(67)% Tb, 10.6(65)% Eu and 0.8(2)% Gd for **9** and 85.2(64)% Eu, 12.8(64)% Gd and 2.0(5)% Tb for **10**. Compounds **8–10** show similar proportions of the lanthanides within the corresponding domains of the products. Each product contains 82–89% of the lanthanide forming the outermost shell, 10–14% of the lanthanide from the middle shell and 1–4% of the lanthanide from the core. This distribution is consistent with expectations given that EDX is a surface analysis technique, so would be expected to be dominated by the outermost shell in each case.

The solid-state fluorescence emission and excitation spectra were recorded for **8–10** at room temperature and are shown in Fig. 8–10 respectively. For each product, emission spectra were recorded by excitation of the ligand at 370 nm and at 254 nm.

Visual observations under a UV lamp (254 nm) show that **8** is pale yellow. Both emission spectra (Fig. 8a) show the presence of peaks corresponding to the energy states of Tb^{3+} (490 nm and 545 nm) and Eu^{3+} transitions (590 nm and 618 nm). The highest intensity peaks are those of the Tb^{3+} transitions, possibly due to the europium being confined to the inner-core of the crystals. This is in contrast to the mixed-lanthanide system **7** which was formed by one-pot reaction and displayed emission spectra dominated by Eu^{3+}. A broad band at 400–500 nm is also present which originates from the ligand.

The excitation spectra were recorded through excitation of the ligand (442 nm), Tb^{3+} (545 nm) and Eu^{3+} (618 nm) (Fig. 8b). Excitation of either Eu^{3+} and Tb^{3+} gave spectra containing a broad, high intensity band from 250–340 nm. This band, also present in the spectra of **2** and **4**, is believed to arise from charge transfer from the ligand to the metal

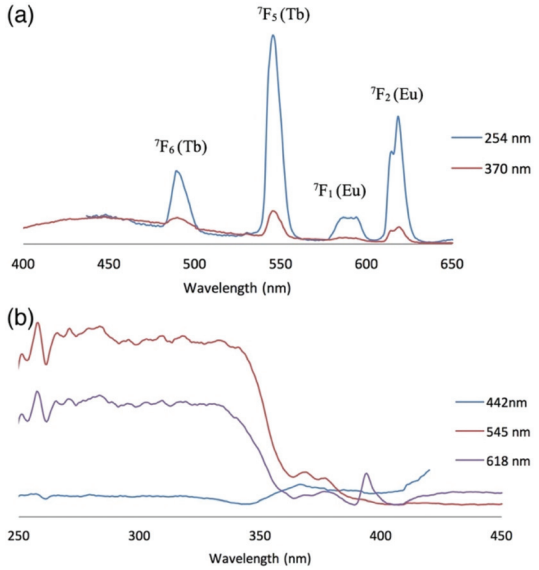

Fig. 8 Solid-state fluorescence (a) emission and (b) excitation spectra for [Gd(Hodip)(H_2O)]@[Tb(Hodip)(H_2O)]@[Eu(Hodip)(H_2O)] **8** at different excitation wavelengths.

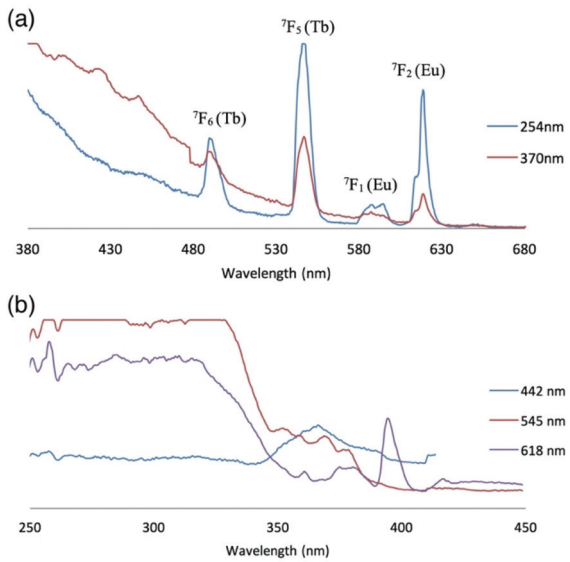

Fig. 9 Solid-state fluorescence (a) emission and (b) excitation spectra for [Tb(Hodip)(H_2O)]@[Eu(Hodip)(H_2O)]@[Gd(Hodip)(H_2O)] **9** at different excitation wavelengths.

centres. In the case of **7**, these bands are high in intensity for both Eu^{3+} (λ_{ex} = 618 nm) and Tb^{3+} (λ_{ex} = 545 nm) excitation, demonstrating that excitation of the core–shell compound between 250 nm–340 nm will result in emissions in both the green (terbium) and red (europium) regions. The band arising from excitation of Tb^{3+} has the higher intensity of the two, supporting the visual observations of an overall pale yellow appearance of **7** under UV excitation. Bands associated with the ligand (370 nm) and Eu^{3+} (394 nm) are also present at a lower intensity.

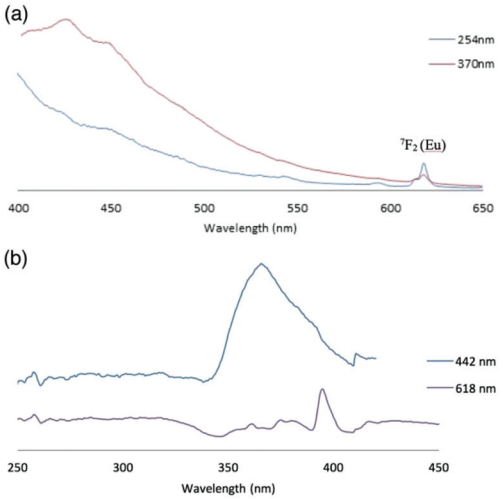

Fig. 10 Solid-state fluorescence (a) emission and (b) excitation spectra for [Eu(Hodip)(H_2O)]@[Gd(Hodip)(H_2O)]@[Tb(Hodip)(H_2O)] **10** at different excitation wavelengths.

Visual observations showed that when irradiated with UV light (254 nm) **9** was pale yellow in appearance. Solid-state fluorescence emission and excitation spectra are comparative to those of **8** with emissions corresponding to the ligand (380–480 nm), Tb^{3+} transitions (490 nm, 545 nm) and Eu^{3+} transitions (587 nm and 618 nm) (Fig. 9a). As with **8**, the higher intensity of the Tb^{3+} transitions is indicative of the core–shell ordering in the material.

The excitation of both Eu^{3+} (λ_{ex} = 618 nm) and Tb^{3+} (λ_{ex} = 545 nm) show the presence of a LMCT band from 250 nm–340 nm (Fig. 9b). Excitation of the ligand (λ_{ex} = 442 nm) is dominated by the band at 370 nm. Overall, the two mixed-lanthanide core–shell structures **8** and **9** show high emission contributions from Eu^{3+} and Tb^{3+} centres. Some changes in relative intensities of the Eu^{3+} and Tb^{3+} emissions can be seen between the two core–shell materials. This demonstrates that segregation of the lanthanide species into single domains within the core–shell structure together with the ordering of the shells allows some degree of control over the emission of the resulting material.

In contrast to **8** and **9**, visual observations on **10** show that the compound appears purple when illuminated with UV light (254 nm). The solid-state fluorescence emission spectra (Fig. 10a) show a broad band from the ligand (400–500 nm) and peaks associated with the Eu^{3+} transitions (593 nm, 618 nm) which accounts for the purple appearance of the compound when irradiated with UV light. No Tb^{3+} transitions are observed in the emission spectra, which is a likely consequence of the Tb^{3+} centres being confined to the innermost shell of the structure rather than energy transfer from Tb^{3+} to Eu^{3+} due to the separation of these lanthanides by the Gd^{3+}-containing layer.

The excitation spectrum recorded at the excitation maximum of the ligand (442 nm) (Fig. 10b) shows bands characteristic of the ligand at 370 nm. Excitation at 618 nm

shows bands from the ligand (370 nm) and Eu^{3+} (394 nm). The predominance of the ligand and europium transitions, to the detriment of those arising from terbium, in **10** contrasts with observations for **8** and **9**, and is consistent with the order of the domains in these systems influencing the fluorescence properties of the core–shell material. Alteration of shell ordering and thickness may therefore be exploited as a means of tailoring the optical properties of core–shell lanthanide MOFs.

Physical mixtures of [Ln(odip)(H_2O)] compounds 2–4

Physical blending of lanthanide compounds in order to produce colour tuneable materials has been demonstrated previously. Therefore, the optical properties of a physical mixture of **2**, **3** and **4** were investigated and compared to those of the mixed-lanthanide MOF **7** and the core–shell MOFs **8–10**. Compounds **2–4** were combined together in a 1 : 1 : 1 ratio post-synthesis. Observations of this mixture under UV irradiation showed the sample to appear green with blue and red speckles (Fig. S7†), indicative of its heterogeneous nature. Solid-state fluorescence emission spectra of the mixture were collected at room temperature using excitation wavelengths of 254 and 370 nm and are shown in Fig. 11a. Both spectra show similar features with bands at 490 nm and 545 nm corresponding to Tb^{3+}, 587 nm and 618 nm corresponding to Eu^{3+}, and the tail end of the broad peak at 390–470 nm typical of the ligand. The highest intensity transitions are those of Tb^{3+}, supporting the green colour of the mixture observed visually.

The excitation spectra recorded at optimal excitation wavelengths of the ligand (442 nm) and Eu^{3+} (618 nm) are shown in Fig. 11b. A broad, high intensity band is present from 250–350 nm along with bands associated with the ligand (370 nm) and Tb^{3+} (394 nm). Both the emission and excitation spectra are similar to those of the core–shell MOFs **8** and **9**, confirming that these mixed-lanthanide MOFs behave in a similar way to the combined single lanthanide systems.

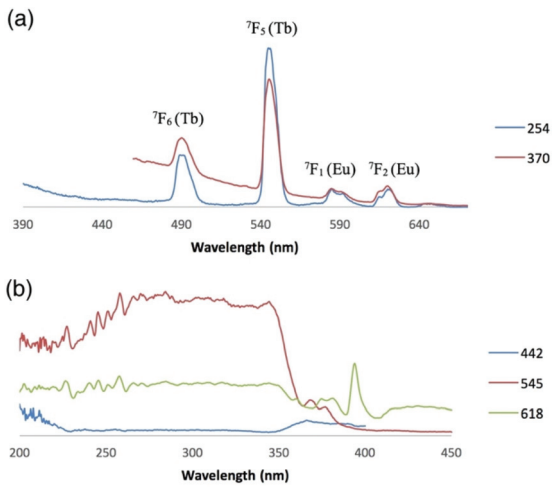

Fig. 11 Solid-state fluorescence (a) emission and (b) excitation spectra for a physical mixture of **2**, **3** and **4** at different excitation wavelengths.

However, in contrast to the heterogeneous appearance of the physical mixture, the core–shell materials exhibit uniform appearance across the sample. This is of particular interest in applications such as light emitting devices which require uniform emission in order to produce an evenly dispersed and stable material.

Conclusions

Lanthanide MOFs of the form [Ln(Hodip)(H_2O)]·$n$$H_2O$ (Ln = Sm, Eu, Gd, Tb, Dy and Er) have been prepared and shown to have isostructural three-dimensional network structures. Using a 1 : 1 : 1 mixture of europium, terbium and gadolinium nitrates in the reaction mixture led to the formation of [$Gd_{0.17}Tb_{0.19}Eu_{0.64}$(Hodip)($H_2O$)]·$n$$H_2O$ **7**. The emission spectrum of **7** is dominated by Eu^{3+} transitions, with the additional presence of lower intensity Tb^{3+} and ligand transitions, and appears red upon excitation with UV light.

Three mixed-lanthanide core–shell MOFs have also been prepared. The fluorescence emission spectra of the Gd@Tb@Eu and Tb@Eu@Gd systems, **8** and **9**, are dominated by terbium(III) emissions, though europium(III) and ligand transitions are also observed. Excitation over a broad wavelength (250–350 nm) results in high intensity emission of both green (Tb) and red (Eu) light. This is advantageous for lanthanide systems as, if the material maintains its emission properties on changing excitation source, it is likely to be more versatile in potential applications.

In contrast, the Eu@Gd@Tb system, **10**, shows an emission spectrum with only Eu^{3+} and ligand transitions present. As the Tb^{3+} and Eu^{3+} domains are separated by the Gd^{3+} layer, quenching of the Tb^{3+} transitions through metal to metal energy transfer cannot be occurring. This suggests that placing the Tb^{3+} centres in the core of the particles is sufficient to ensure that their emission is not observable. The ordering and thickness of the domains in core–shell structures clearly influences the optical properties of the resulting material. This is likely to provide a route to emission colour tailoring of lanthanide MOFs, and this is the subject of current investigations.

Conflicts of interest

There are no conflicts of interest to declare.

Acknowledgements

The EPSRC is thanked for a PhD studentship to LKC.

Notes and references

1 K. Müller-Buschbaum, in *The Chemistry of Metal-Organic Frameworks*, ed. S. Kaskel, Wiley-VCH, Weinheim, 2016, vol. 1, p. 231.

2 S. Fordham, X. Wang, M. Bosch and H.-C. Zhou, *Struct. Bonding*, 2015, **163**, 1.
3 M. D. Allendorf, C. A. Bauer, R. K. Bhakta and R. J. Houk, *Chem. Soc. Rev.*, 2009, **38**, 1330.
4 Y. Cui, Y. Yue, G. Qian and B. Chen, *Chem. Rev.*, 2012, **112**, 1126.
5 X.-Z. Song, S.-Y. Song and H.-J. Zhang, *Struct. Bonding*, 2015, **163**, 109.
6 S. Dang, J.-H. Zhang, Z.-M. Sun and H. Zhang, *Chem. Commun.*, 2012, **48**, 11139.
7 Y. Cui, H. Xu, Y. Yue, Z. Guo, J. Yu, Z. Chen, J. Gao, Y. Yang, G. Qian and B. Chen, *J. Am. Chem. Soc.*, 2012, **134**, 3979.
8 X. Rao, T. Song, J. Gao, Y. Cui, Y. Yang, C. Wu, B. Chen and G. Qian, *J. Am. Chem. Soc.*, 2013, **135**, 15559.
9 G. E. Gomez, A. M. Kaczmarek, R. Van Deun, E. V. Brusau, G. E. Narda, D. Vega, M. Iglesias, E. Gutiérrez-Puebla and M. A. Monge, *Eur. J. Inorg. Chem.*, 2016, **2016**, 1577.
10 R.-Z. Wu, X. Yang, L.-W. Zhang and P.-P. Zhou, *Dalton Trans.*, 2017, **46**, 9859.
11 H. Xu, C.-S. Cao and B. Zhao, *Chem. Commun.*, 2015, **51**, 10280.
12 I. A. Ibarra, T. W. Hesterberg, J.-S. Chang, J. W. Yoon, B. J. Holliday and S. M. Humphrey, *Chem. Commun.*, 2013, **49**, 7156.
13 S. G. Dunning, A. J. Nuñez, M. D. Moore, A. Steiner, V. M. Lynch, J. L. Sessler, B. J. Holliday and S. M. Humphrey, *Chem*, 2017, **2**, 579.
14 V. Haquin, M. Etienne, C. Daiguebonne, S. Freslon, G. Calvez, K. Bernot, L. Le Pollès, S. E. Ashbrook, M. R. Mitchell, J.-C. Bünzli, S. V. Eliseeva and O. Guillou, *Eur. J. Inorg. Chem.*, 2013, **2013**, 3464.
15 L. V. Meyer, F. Schönfeld and K. Müller-Buschbaum, *Chem. Commun.*, 2014, **50**, 8093.
16 K. A. White, D. A. Chengelis, K. A. Gogick, J. Stehman, N. L. Rosi and S. Petoud, *J. Am. Chem. Soc.*, 2009, **131**, 18069.
17 H. Furukawa, K. E. Cordova, M. O'Keeffe and O. M. Yaghi, *Science*, 2013, **341**, 1230444.
18 A. D. Burrows, *CrystEngComm*, 2011, **13**, 3623.
19 H. Guo, Y. Zhu, S. Qiu, J. A. Lercher and H. Zhang, *Adv. Mater.*, 2010, **22**, 4190.
20 S.-M. Li, X.-J. Zheng, D.-Q. Yuan, A. Ablet and L.-P. Jin, *Inorg. Chem.*, 2012, **51**, 1201.
21 M.-L. Ma, C. Ji and S.-Q. Zang, *Dalton Trans.*, 2013, **42**, 10579.
22 Q. Tang, S. Liu, Y. Liu, D. He, J. Miao, X. Wang, Y. Ji and Z. Zheng, *Inorg. Chem.*, 2014, **53**, 289.
23 L. L. da Luz, B. F. Lucena Viana, G. C. O. da Silva, C. C. Gatto, A. M. Fontes, M. Malta, I. T. Weber, M. O. Rodrigues and S. A. Júnior, *CrystEngComm*, 2014, **16**, 6914.
24 S. Su, W. Chen, C. Qin, S. Song, Z. Guo, G. Li, X. Song, M. Zhu, S. Wang, Z. Hao and H. Zhang, *Cryst. Growth Des.*, 2012, **12**, 1808.
25 Y. Peng, G. Li, J. Hua, Z. Shi and S. Feng, *CrystEngComm*, 2015, **17**, 3162.
26 H. Guo, Y. Yan, X. Guo, N. Wang and Y. Qi, *J. Mol. Struct.*, 2016, **1108**, 134.
27 J. Bernstein, R. E. Davis, L. Shimoni and N. L. Chang, *Angew. Chem., Int. Ed. Engl.*, 1995, **34**, 1555.
28 S. Lis, *Acta Phys. Pol., A*, 1993, **84**, 1003.
29 V. Zolin, L. Puntus, V. Kudryashova, V. Tsaryuk, J. Legendziewicz, P. Gawryszewska and R. Szostak, *J. Alloys Compd.*, 2002, **341**, 376.